

# **Supplementary Information of the research article:**

## **Resolving the central metabolism of Arabidopsis guard cells**

Semidán Robaina-Estévez<sup>1\*</sup>, Danilo de Menezes Daloso<sup>2,3\*</sup>, Youjun Zhang<sup>2</sup>, Alisdair R. Fernie<sup>2</sup>, Zoran Nikoloski<sup>1\*\*</sup>

<sup>1</sup>Systems Biology and Mathematical Modeling Group, Max Planck Institute of Molecular Plant Physiology, Potsdam-Golm, Germany, <sup>2</sup>Bioinformatics Group, Institute of Biochemistry and Biology, University of Potsdam, Potsdam-Golm, Germany, <sup>3</sup>Central Metabolism Group, Max Planck Institute of Molecular Plant Physiology, Potsdam-Golm, Germany, <sup>4</sup>Departamento de Bioquímica e Biologia Molecular, Universidade Federal do Ceará, Fortaleza-CE, Brasil

\*these authors contributed equally

\*\*corresponding author: nikoloski@mpimp-golm.mpg.de

## **Contents**

Supplementary Tables S1 to S12

Supplementary Figure S1

Supplementary Appendix S1

**Table S1. A comparison of the predicted metabolic state of GC and M.** The predicted mean flux values corresponding to the reactions depicted in Figure 1 are shown for G and M cells. The p-values shown in this table correspond to a Mann-Whitney test comparing the distributions of flux values of G and M cells ( $V_G$  and  $V_M$ , respectively). Three different tests were considered for each comparison: (i) we evaluated whether the two distributions differ (null hypothesis  $H_0: V_G = V_M$ ), (ii) if G had increased flux values in comparison to M cells ( $H_0: V_M > V_G$ ), and (iii) if M had increased flux values in comparison to G cells ( $H_0: V_G > V_M$ ). In all three cases, a horizontal bar indicates a failure of the test due to distributions consisting of a fixed value. Reaction names and index numbers in accord with AraCOREd.

Idx. in Fig.1	Reaction Name (Idx in AraCOREd)	Mean Flux G	Mean Flux M	Mean ratio (G/M)	Ho: $V_G = V_M$	Ho: $V_M > V_G$	Ho: $V_G > V_M$	SubSystem
PSII	photosystem II (1)	0.125	0.125	1.000	0.317	0.159	0.841	light reactions
Cb6f	cytochrom b6f complex (2)	0.250	0.250	1.000	0.317	0.159	0.841	light reactions
PSI	photosystem I (3)	0.500	0.500	1.000	0.317	0.159	0.841	light reactions
ATPase	ATPase (5)	0.107	0.107	1.000	0.317	0.159	0.841	light reactions
1	PEP carboxylase (54)	0.420	0.034	12.486	0	0	1.000	gluconeogenesis
2	Cytosolic NADP-MDH (115)	0.161	0.084	1.917	0	0	1.000	pyruvate metabolism
3	Dicarboxylate transporter (339)	0.251	0.033	7.554	0	0	1.000	transport
4	Plastidial NADP-Malic Enzyme (113)	0.249	0.032	7.848	0	0	1.000	pyruvate metabolism
5	CO2 diffusion [Forward] (374)	0	0.001	0	0	1.000	0	transport
5	CO2 diffusion [Backward] (374)	0.230	0.013	17.342	0	0	1.000	transport
6	Import CO2 (413)	0.021	0.021	1.000	0.013	0.994	0.006	import
7	Carbonic anhydrase (152)	0.420	0.034	12.486	0	0	1.000	carbon fixation
8	Glu tamate synthase (FeS-Fd) (179)	0.124	3.671e-05	3.391e+03	0	0	1.000	glutamate synthesis
9	Ferredoxin-NADP reductase (4)	0.126	0.250	0.502	0	1.000	0	light reactions
10	Export O2 (420)	0.020	0.020	1.000	0.847	0.424	0.576	export
11	TP isomerase [Forward] (9)	0.854	0.855	0.999	0	1.000	0	Calvin-Benson cycle, glycolysis
12	TP/Pi translocator [Forward] (328)	0.857	1.000	0.858	0	1.000	0	transport
13	Di-/ri-carboxylate carrier [Forward] (346)	0.348	0.327	1.065	0	0	1.000	transport
13	Di-/ri-carboxylate carrier [Forward] (347)	0.345	0.324	1.065	0	0	1.000	transport
13	Di-/ri-carboxylate carrier [Forward] (348)	0.349	0.324	1.077	0	0	1.000	transport
14	Di-/ri-carboxylate carrier [Backward] (343)	0.311	0.294	1.059	0	0	1.000	transport
14	Di-/ri-carboxylate carrier [Backward] (344)	0.314	0.289	1.088	0	0	1.000	transport
14	Di-/ri-carboxylate carrier [Backward] (345)	0.309	0.292	1.057	2.395e-06	1.198e-06	1.000	transport
15	Mitochondrial NAD-MDH [Backward] (80)	0.271	0.226	1.201	0	0	1.000	tricarboxylic acid cycle, glyoxylate cycle
15	Mitochondrial NADP-MDH (117)	0.753	0.724	1.041	0	0	1.000	pyruvate metabolism
16	FBP aldolase [Forward] (35)	0.018	0.160	0.112	0	1.000	0	sucrose synthesis, gluconeogenesis, glycolysis
17	FBPase (36)	0.073	0	inf	0	0	1.000	sucrose synthesis, gluconeogenesis, glycolysis
17	PPi-dep. Phosphofruktokinase [Backward] (136)	0	0.693	0	0	1.000	0	pyrophosphate recycling
18	G6P isomerase [Forward] (39)	0.018	0.160	0.112	0	1.000	0	sucrose synthesis, sucrose degradation, gluconeogenesis
19	Phosphoglucomutase [Forward] (40)	0.055	7.590e-04	72.503	0	0	1.000	sucrose synthesis, sucrose degradation
20	TP/Pi translocator [Forward] (327)	0	0	0	-	-	-	transport
20	TP/Pi translocator [Backward] (327)	0.362	0.439	0.825	0	1.000	0	transport

**Table S2. Predicted Flux-Sums of selected metabolites in the AraCOREred model.** The predicted mean flux-sum values for several metabolites are displayed. In each of the metabolites, the flux-sum values are split into each cellular compartment: cytosol (c), mitochondrion (m), peroxisome (p) and chloroplast (h). In addition, the total flux-sum values (*i.e.*, taking into account all the compartments) are provided. The interpretation of the p-values is similar to that of Table S1. A horizontal bar indicates a failure of the test due to distributions consisting of a fixed value.

Metabolite (compartment)	Mean FluxSum G	Mean FluxSum M	Ratio (G/M)	Ho: $V_G = V_M$	Ho: $V_M > V_G$	Ho: $V_G > V_M$
Total Mal	5.434	4.581	1.186	0	0	1.000
Mal(c)	2.451	2.172	1.128	0	0	1.000
Mal(m)	2.129	2.004	1.062	0	0	1.000
Mal(p)	0	0	-	-	-	1.000
Mal(h)	2.211	1.493	1.481	0	0	1.000
Total Suc	0.109	5.574e-05	1.948e+03	0	0	1.000
Futile Cycle Suc	0.109	1.203e-05	9.019e+03	0	1.000	0
Total OAA	7.460	6.729	1.109	0	0	1.000
OAA(c)	4.063	3.606	1.127	0	0	1.000
OAA(m)	2.083	1.950	1.069	0	0	1.000
OAA(p)	1.320	1.488	0.887	0	1.000	0
OAA(h)	1.713	1.430	1.198	0	0	1.000
Total Pyr	3.571	3.085	1.158	0	0	1.000
Pyr(c)	1.418	1.344	1.055	0	0	1.000
Pyr(h)	0.498	0.139	3.574	0	0	1.000
Pyr(m)	1.656	1.639	1.010	0	0	1.000
Pyr(p)	1.418	1.268	1.118	0	0	1.000
Total PEP	2.896	2.583	1.121	0	0	1.000
PEP(c)	1.880	1.679	1.120	0	0	1.000
PEP(h)	1.536	1.672	0.919	0	1.000	0
G3P(h)	3.626	2.832	1.280	0	0	1.000
G3P(c)	1.837	0.966	1.901	0	0	1.000
Total ATP	1.967	1.609	1.223	0	0	1.000
ATP(h)	1.050	1.050	1.000	0	0	1.000
ATP(c)	6.691	6.234	1.073	0	0	1.000
ATP(m)	3.445	3.349	1.028	0	0	1.000
Total NADP	1.740	1.437	1.211	0	0	1.000
NADP(h)	1.506	1.447	1.041	0	0	1.000
NADP(c)	6.691	6.234	1.073	0	0	1.000
NADP(m)	3.445	3.349	1.028	0	0	1.000
Total NADPH	1.740	1.437	1.211	0	0	1.000
NADPH(h)	1.506	1.447	1.041	0	0	1.000
NADPH(c)	2.781	1.659	1.677	0	0	1.000
NADPH(m)	2.171	1.602	1.355	0	0	1.000
Total CO <sub>2</sub>	0.839	0.070	11.998	0	0	1.000
CO <sub>2</sub> (h)	0.001	0.002	0.788	0	1.000	0
CO <sub>2</sub> (c)	5.434	4.581	1.186	0	0	1.000
CO <sub>2</sub> (m)	2.451	2.172	1.128	0	0	1.000

**Table S3. Activity of the CBC and starch metabolism in GC and M.** The predicted mean flux values of reactions in the CBC cycle and starch metabolism are shown for G and M cells. The interpretation of the p-values is similar to that of Table S1. A horizontal bar indicates a failure of the test due to distributions consisting of a fixed value. Reaction names and index numbers in accord with AraCOREred.

Reaction [direction](Idx in AraCOREred)	Mean Flux G	Mean Flux M	Mean ratio (G/M)	Ho: $V_G = V_M$	Ho: $V_M > V_G$	Ho: $V_G > V_M$
<b>CBC</b>						
RuBisCO Carboxylation (6)	0.019	0.020	0.974	0	1.000	0
RuBisCO Oxygenation( 85)	2.043e-06	2.043e-06	1.000	0	0	1.000
PGA kinase [Forward] (7)	0.495	0.278	1.779	0	0	1.000
GAP dehydrogenase (8)	0.864	0.959	0.901	0	1.000	0
TP isomerase [Forward] (9)	0.854	0.855	0.999	0	1.000	0
FBP aldolase [Forward] (10)	0	0	0	-	-	-
FBPase (11)	0	0	0	-	-	-
F6P transketolase (12)	0.007	0.007	0.974	0	1.000	0
SBP aldolase (13)	0	0	0	-	-	-
SBPase (14)	0	0	0	-	-	-
S7P transketolase (15)	0.006	0.007	0.974	0	1.000	0
Ru5P epimerase (16)	0.013	0.013	0.974	0	1.000	0
R5P isomerase (17)	0.006	0.007	0.973	0	1.000	0
Ru5P kinase (18)	0.019	0.020	0.974	0	1.000	0
PGA kinase [Backward] (7)	0	0	0	-	-	-
TP isomerase [Backward] (9)	0	0	0	-	-	-
FBP aldolase [Backward] (10)	0.004	0.145	0.025	0	1.000	0
<b>Starch metabolism</b>						
starch synthase (22)	2.949e-04	2.949e-04	1.000	0	0	1.000
starch synthase (23)	2.975e-04	3.068e-04	0.970	0	1.000	0
starch synthase (24)	2.610e-06	1.177e-05	0.222	0	1.000	0
amylase (26)	2.610e-06	2.107e-05	0.124	0	1.000	0
disproportionating enzyme (28)	0	9.165e-06	0	0	1.000	0
disproportionating enzyme (29)	0	9.298e-06	0	0	1.000	0

**Table S4. A comparison of the maximum alternative optimal flux values of G and M cells for the reactions depicted in Figure 1.** Results derived from the Flux Variability Analysis applied to the alternative optima space of RegrEx:  $V_{\max}G$ ,  $V_{\max}M$ , the maximum flux value in the alternative optima space (as calculated by RegrEx<sub>FVA</sub>) in G and M cells, respectively, and their difference are included. The p-values shown in this table correspond to a Mann-Whitney test comparing the distributions of flux values of G and M cells ( $V_G$  and  $V_M$ , respectively).

Idx. in Fig.1	Reaction Name (Idx in AraCOREd)	$V_{\max}G$	$V_{\max}M$	$V_{\max}G - V_{\max}M$	Ho: $V_G > V_M$	SubSystem
PSII	photosystem II (1)	0.125	0.125	0	0.841	light reactions
Cb6f	cytochrom b6f complex (2)	0.250	0.250	0	0.841	light reactions
PSI	photosystem I (3)	0.500	0.500	0	0.841	light reactions
ATPase	ATPase (5)	0.107	0.107	0	0.841	light reactions
1	PEP carboxylase (54)	0.466	0.054	0.412	1.000	gluconeogenesis
2	Cytosolic NADP-MDH (115)	0.168	0.105	0.063	1.000	pyruvate metabolism
3	Dicarboxylate transporter (339)	0.255	0.054	0.201	1.000	transport
4	Plastidial NADP-Malic Enzyme (113)	0.254	0.053	0.201	1.000	pyruvate metabolism
5	CO2 diffusion [Forward] (374)	1.000 e-06	0.012	-1.158e-02	0	transport
5	CO2 diffusion [Backward] (374)	0.234	0.033	0.201	1.000	transport
6	Import CO2 (413)	0.021	0.021	4.950e-05	0.006	import
7	Carbonic anhydrase (152)	0.466	0.054	0.412	1.000	carbon fixation
8	Glu synthase (FeS-Fd) (179)	0.250	0.026	0.224	1.000	glutamate synthesis
9	ferredoxin-NADP reductase (4)	0.235	0.250	-1.529e-02	0	light reactions
10	Export O2 (420)	0.020	0.020	1.310e-04	0.576	export
11	TP isomerase [Forward] (9)	0.874	0.924	-5.007e-02	0	Calvin-Benson cycle, glycolysis
12	TP/Pi translocator [Forward] (328)	0.888	1.000	-1.117e-01	0	transport
13	Di-/ri-carboxylate carrier [Forward] (346)	1.000	1.000	0	1.000	transport
13	Di-/ri-carboxylate carrier [Forward] (347)	1.000	1.000	0	1.000	transport
13	Di-/ri-carboxylate carrier [Forward] (348)	1.000	1.000	0	1.000	transport
14	Di-/ri-carboxylate carrier [Backward] (343)	1.000	1.000	0	1.000	transport
14	Di-/ri-carboxylate carrier [Backward] (344)	1.000	1.000	0	1.000	transport
14	Di-/ri-carboxylate carrier [Backward] (345)	1.000	1.000	0	1.000	transport
15	Mitochondrial NAD-MDH [Backward] (80)	0.323	0.323	-4.698e-04	1.000	tricarboxylic acid cycle, glyoxylate cycle
15	Mitochondrial NADP-MDH (117)	0.769	0.746	0.023	1.000	pyruvate metabolism
16	FBP aldolase [Forward] (35)	0.034	0.218	-1.839e-01	0	sucrose synthesis, gluconeogenesis, glycolysis
17	FBPase (36)	0.090	0.006	0.083	1.000	sucrose synthesis, gluconeogenesis, glycolysis
17	PPi-dep. Phosphofructokinase [Backward] (136)	1.000 e-06	0.695	-6.950e-01	0	pyrophosphate recycling
18	G6P isomerase [Forward] (39)	0.034	0.218	-1.839e-01	0	sucrose synthesis, sucrose degradation, gluconeogenesis
19	Phosphoglucomutase [Forward] (40)	0.057	0.003	0.054	1.000	sucrose synthesis, sucrose degradation
20	TP/Pi translocator [Forward] (327)	1.000 e-06	1.000e-06	0	1.000	transport
20	TP/Pi translocator [Backward] (327)	0.386	0.600	-2.147e-01	0	transport

**Table S5. A comparison of the maximum alternative optimal flux values of G and M cells for the reactions in the CBC and starch metabolism.** Results derived from the Flux Variability Analysis applied to the alternative optima space of ReGrEx:  $V_{\max}G$ ,  $V_{\max}M$ , the maximum flux value in the alternative optima space (as calculated by ReGrEx<sub>FVA</sub>) in G and M cells, respectively, and their difference are included. The p-values shown in this table correspond to a Mann-Whitney test comparing the distributions of flux values of G and M cells ( $V_G$  and  $V_M$ , respectively).

Reaction [direction](Idx in GEM)	$V_{\max}G$	$V_{\max}M$	$V_{\max}G - V_{\max}M$	Ho: $V_G > V_M$
<b>CBC</b>				
RuBisCO Carboxylation (6)	0.021	0.023	-1.784e-03	0
RuBisCO Oxygenation( 85)	2.514e-04	2.661e-04	-1.467e-05	-
PGA kinase [Forward] (7)	0.500	0.299	0.201	1.000
GAP dehydrogenase (8)	0.911	0.963	-5.196e-02	0
TP isomerase [Forward] (9)	0.874	0.924	-5.007e-02	0
FBP aldolase [Forward] (10)	0.005	1.000e-06	0.005	1.000
FBPase (11)	0.005	0.005	1.373e-04	1.96E-01
F6P transketolase (12)	0.007	0.008	-5.059e-04	0
SBP aldolase (13)	0.005	0.006	-8.402e-04	0
SBPase (14)	0.005	0.006	-8.402e-04	0
S7P transketolase (15)	0.007	0.008	-5.058e-04	0
Ru5P epimerase (16)	0.014	0.015	-1.012e-03	0
R5P isomerase (17)	0.007	0.007	-5.058e-04	0
Ru5P kinase (18)	0.021	0.023	-1.784e-03	0
PGA kinase [Backward] (7)	1.000e-06	1.000e-06	0	-
TP isomerase [Backward] (9)	1.000e-06	1.000e-06	0	0
FBP aldolase [Backward] (10)	0.020	0.204	-1.838e-01	0
<b>Starch metabolism</b>				
starch synthase (22)	0.020	0.204	-1.838e-01	1.000
starch synthase (23)	0.002	0.002	6.434e-04	0
starch synthase (24)	0.005	0.006	-7.696e-04	0
amylase (26)	0.004	0.003	0.001	0
disproportionating enzyme (28)	0.004	0.003	0.001	0
disproportionating enzyme (29)	0.004	0.003	0.001	0
disproportionating enzyme (30)	0.004	0.003	0.001	1.76E-05
(starch) phosphorylase (32)	0.002	0.002	1.543e-04	1.000

**Table S6. A comparison of the predicted metabolic state of G and M cells after imposing additional experimental constraints.** This table shows the analogous results, presented in Table S1, when additional constraints are taken in consideration. Concretely, the carboxylation to oxygenation ratio of RubisCO is constrained to stay within 1.5 and 4. Additionally, the flux through the reactions in the CBC: the *sedoheptulose 1,7-bisphosphate aldolase* and the *sedoheptulose-1,7-bisphosphatase* is constrained to carry a positive flux (Details in Materials & Methods). A horizontal bar indicates a failure of the test due to distributions consisting of a fixed value. Reaction names and index numbers in accord with AraCOREd.

Idx in Fig 1	Reaction Name (Idx in AraCOREd)	Mean Flux G	Mean Flux M	Mean ratio (G/M)	Ho: $V_G = V_M$	Ho: $V_M > V_G$	Ho: $V_G > V_M$	SubSystem
PSII	photosystem II (1)	0.125	0.125	1.000	-	-	-	light reactions
Cb6f	cytochrom b6f complex (2)	0.250	0.250	1.000	-	-	-	light reactions
PSI	photosystem I (3)	0.500	0.500	1.000	-	-	-	light reactions
ATPase	ATPase (5)	0.107	0.107	1.000	-	-	-	light reactions
1	PEP carboxylase (54)	0.420	0.011	37.190	0	0	1.000	gluconeogenesis
2	Mal dehydrogenase (115)	0.161	0.086	1.866	0	0	1.000	pyruvate metabolism
3	Dicarboxylate transporter (339)	0.223	0.011	19.971	0	0	1.000	transport
4	Mal dehydrogenase (113)	0.221	0.009	24.697	0	0	1.000	pyruvate metabolism
5	CO2 diffusion [Forward] (374)	0	0.013	0	0	1.000	0	transport
5	CO2 diffusion [Backward] (374)	0.199	7.085e-08	2.812e+06	0	0	1.000	transport
6	Import CO2 (413)	0.021	0.021	1.000	0	1.000	0	import
7	HCO3 dehydratase (152)	0.420	0.011	37.190	0	0	1.000	carbon fixation
8	Glu synthase (FeS-Fd) (179)	0.120	1.670e-04	719.020	0	0	1.000	glutamate synthesis
9	ferredoxin-NADP reductase (4)	0.130	0.250	0.520	0	1.000	0	light reactions
10	Export O2 (420)	0.020	0.020	1.000	0	1.000	0	export
11	TP isomerase [Forward] (9)	0.854	0.825	1.035	0	0	1.000	Calvin-Benson cycle, glycolysis
12	TP/Pi translocator [Forward] (328)	0.856	1.000	0.856	0	1.000	0	transport
13	Di-/ri-carboxylate carrier [Forward] (346)	0.362	0.335	1.079	0	0	1.000	transport
13	Di-/ri-carboxylate carrier [Backward] (346)	0.355	0.335	1.060	0	0	1.000	transport
13	Di-/ri-carboxylate carrier [Forward] (347)	0.362	0.338	1.069	0	0	1.000	transport
13	Di-/ri-carboxylate carrier [Backward] (347)	0.332	0.309	1.076	0	0	1.000	transport
13	Di-/ri-carboxylate carrier [Forward] (348)	0.327	0.310	1.056	1.455e-05	7.273e-06	1.000	transport
13	Di-/ri-carboxylate carrier [Backward] (348)	0.332	0.305	1.089	0	0	1.000	transport
14	Di-/ri-carboxylate carrier [Forward] (343)	0.249	0.208	1.199	0	0	1.000	transport
14	Di-/ri-carboxylate carrier [Backward] (343)	0.753	0.720	1.046	0	0	1.000	transport
14	Di-/ri-carboxylate carrier [Forward] (344)	0.022	0.194	0.113	0	1.000	0	transport
14	Di-/ri-carboxylate carrier [Backward] (344)	0.058	0	inf	0	0	1.000	transport
14	Di-/ri-carboxylate carrier [Forward] (345)	0	0.693	0	0	1.000	0	transport
14	Di-/ri-carboxylate carrier [Backward] (345)	0.022	0.194	0.113	0	1.000	0	transport
15	Mal dehydrogenase [Backward] (80)	0.036	7.590e-04	47.157	0	0	1.000	tricarboxylic acid cycle, glyoxylate cycle
15	Mal dehydrogenase (117)	0	0	0	-	-	-	pyruvate metabolism
16	FBP aldolase [Forward] (35)	0.394	0.405	0.973	0	1.000	0	sucrose synthesis, gluconeogenesis, glycolysis
17	FBPase (36)	0.125	0.125	1.000	-	-	-	sucrose synthesis, gluconeogenesis, glycolysis
17	PPi-dep. Phosphofruktokinase [Backward] (136)	0.250	0.250	1.000	-	-	-	pyrophosphate recycling
18	G6P isomerase [Forward] (39)	0.500	0.500	1.000	-	-	-	sucrose synthesis, sucrose degradation, gluconeogenesis
19	Phosphoglucomutase [Forward] (40)	0.107	0.107	1.000	-	-	-	sucrose synthesis, sucrose degradation
20	TP/Pi translocator [Forward] (327)	0.420	0.011	37.190	0	0	1.000	transport
20	TP/Pi translocator [Backward] (327)	0.161	0.086	1.866	0	0	1.000	transport

**Table S7. Activity of the CBC and starch metabolism in G and M cells after imposing additional experimental constraints.** This table shows the analogous results to that of Table S3, when additional constraints are taken in consideration. Concretely, the carboxylation to oxygenation ratio of RubisCO is constrained to stay within 1.5 and 4. Additionally, the flux through the reactions in the CBC: the *sedoheptulose 1,7-bisphosphate aldolase* and the *sedoheptulose-1,7-bisphosphatase* is constrained to carry a positive flux (Details in Materials & Methods). A horizontal bar indicates a failure of the test due to distributions consisting of a fixed value. Reaction names and index numbers in accord with AraCOREd.

Reaction [direction](Idx in GEM)	Mean Flux G	Mean Flux M	Mean ratio (G/M)	Ho: $V_G = V_M$	Ho: $V_M > V_G$	Ho: $V_G > V_M$
<b>CBC</b>						
RuBisCO Carboxylation (6)	0.022	0.022	1.000	0	1.000	0
RuBisCO Oxygenation( 85)	0.005	0.005	1.000	0	1.000	0
PGA kinase [Forward] (7)	0.467	0.255	1.832	0	0	1.000
GAP dehydrogenase (8)	0.864	0.959	0.901	0	1.000	0
TP isomerase [Forward] (9)	0.854	0.825	1.035	0	0	1.000
FBP aldolase [Forward] (10)	5.544e-04	0	Inf	0	0	1.000
FBPase (11)	0.001	0.001	1.000	-	-	-
F6P transketolase (12)	0.009	0.009	1.000	0	1.000	0
SBP aldolase (13)	0.001	0.001	1.000	-	-	-
SBPase (14)	0.001	0.001	1.000	-	-	-
S7P transketolase (15)	0.009	0.009	1.000	0	1.000	0
Ru5P epimerase (16)	0.018	0.018	1.000	0	1.000	0
R5P isomerase (17)	0.009	0.009	1.000	0	1.000	0
Ru5P kinase (18)	0.027	0.027	1.000	0	1.000	0
PGA kinase [Backward] (7)	0	0	0	-	-	-
TP isomerase [Backward] (9)	0	0	0	-	-	-
FBP aldolase [Backward] (10)	0.004	0.176	0.021	0	1.000	0
<b>Starch metabolism</b>						
starch synthase (22)	2.949e-04	2.949e-04	1.000	0	0	1.000
starch synthase (23)	2.975e-04	3.065e-04	0.971	0	1.000	0
starch synthase (24)	2.632e-06	1.203e-05	0.219	0	1.000	0
amylase (26)	2.632e-06	2.106e-05	0.125	0	1.000	0
disproportionating enzyme (28)	2.239e-08	9.423e-06	0.002	0	1.000	0
disproportionating enzyme (29)	0	9.031e-06	0	0	1.000	0

**Table S8. Predicted Flux-Sums of selected metabolites in the AraCOREd model after imposing additional experimental constraints.** This table presents the analogous results of Table S2 when additional constraints are taken in consideration. Concretely, the carboxylation to oxygenation ratio of RubisCO is constrained to stay within 1.5 and 4. Additionally, the flux through the reactions in the CBC: the *sedoheptulose 1,7-bisphosphate aldolase* and the *sedoheptulose-1,7-bisphosphatase* is constrained to carry a positive flux (Details in Materials & Methods).

Metabolite (compartment)	Mean FluxSum G	Mean FluxSum M	Ratio (G/M)	Ho: $V_G = V_M$	Ho: $V_M > V_G$	Ho: $V_G > V_M$
Total Mal	5.615	4.722	1.189	0	0	1.000
Mal(c)	2.678	2.359	1.135	0	0	1.000
Mal(m)	2.355	2.186	1.077	0	0	1.000
Mal(p)	0.006	0.006	1.001	0	1.000	0
Mal(h)	2.155	1.443	1.493	0	0	1.000
Total Suc	0.070	5.574e-05	1.258e+03	0	0	1.000
Futile Cycle Suc	0.070	1.203e-05	5.822e+03	0	1.000	0
Total OAA	7.570	6.777	1.117	0	0	1.000
OAA(c)	4.191	3.677	1.140	0	0	1.000
OAA(m)	2.156	2.017	1.069	0	0	1.000
OAA(p)	1.326	1.494	0.888	0	1.000	0
OAA(h)	1.713	1.425	1.202	0	0	1.000
Total Pyr	3.510	2.980	1.178	0	0	1.000
Pyr(c)	1.413	1.303	1.084	0	0	1.000
Pyr(h)	0.442	0.057	7.725	0	0	1.000
Pyr(m)	1.656	1.639	1.010	0	0	1.000
Pyr(p)	1.413	1.264	1.117	0	0	1.000
Total PEP	2.926	2.542	1.151	0	0	1.000
PEP(c)	1.937	1.679	1.154	0	0	1.000
PEP(h)	1.538	1.672	0.920	0	1.000	0
G3P(h)	3.348	2.539	1.318	0	0	1.000
G3P(c)	1.693	0.845	2.003	0	0	1.000
Total ATP	1.802	1.417	1.271	0	0	1.000
ATP(h)	0.968	0.968	1.000	0	0	1.000
ATP(c)	6.691	6.226	1.075	0	0	1.000
ATP(m)	3.445	3.344	1.030	0	0	1.000
Total NADP	1.740	1.442	1.207	0	0	1.000
NADP(h)	1.506	1.440	1.046	0	0	1.000
NADP(c)	6.691	6.226	1.075	0	0	1.000
NADP(m)	3.445	3.344	1.030	0	0	1.000
Total NADPH	1.740	1.442	1.207	0	0	1.000
NADPH(h)	1.506	1.440	1.046	0	0	1.000
NADPH(c)	2.759	1.619	1.704	0	0	1.000
NADPH(m)	2.116	1.580	1.339	0	0	1.000
Total CO <sub>2</sub>	0.839	0.048	17.473	0	0	1.000
CO <sub>2</sub> (h)	0.007	0.007	1.000	0	1.000	0
CO <sub>2</sub> (c)	5.615	4.722	1.189	0	0	1.000
CO <sub>2</sub> (m)	2.678	2.359	1.135	0	0	1.000

**Table S9. Redistribution of the percentage of <sup>13</sup>C label enrichment in primary metabolites.** M and G cells were fed with <sup>13</sup>-NaHCO<sub>3</sub> and harvested after 30 min and 60 min in the light. Values in bold and underline type are significantly different between M and G cells according to Students *t*-test (*P* < 0.05) in the same time point. Data presented are mean ± SE (*n* = 3).

Metabolite	m/z	% of <sup>13</sup> C enrichment							
		M30	SE	M60	SE	GC30	SE	GC60	SE
Gly	102	0.010	0.004	0.005	0.001	0.015	0.003	0.006	0.002
Ser	306	0.016	0.014	0.009	0.005	0.007	0.004	<b><u>0.036</u></b>	<b><u>0.004</u></b>
Ser	204	0.101	0.052	0.060	0.020	0.111	0.036	0.097	0.007
Homoserine	128	0.449	0.272	0.380	0.028	0.282	0.124	0.332	0.237
Glycolate	205	0.008	0.008	0.007	0.007	0.015	0.008	0.017	0.008
Val	218	0.240	0.180	0.095	0.091	0.051	0.027	0.162	0.035
Ala	188	0.416	0.198	0.361	0.141	1.476	1.260	0.459	0.355
Thr	219	0.458	0.238	0.342	0.132	0.795	0.330	0.634	0.067
Thr	291	0.927	0.438	0.748	0.260	1.489	0.447	<b><u>1.361</u></b>	<b><u>0.118</u></b>
Pro	142	0.197	0.100	0.164	0.021	0.321	0.151	<b><u>0.367</u></b>	<b><u>0.012</u></b>
Asp	218	0.018	0.018	0.012	0.012	<b><u>1.638</u></b>	<b><u>0.947</u></b>	0.786	0.622
Asp	232	0.045	0.004	0.037	0.002	<b><u>0.078</u></b>	<b><u>0.005</u></b>	0.038	0.001
Leu	158	0.034	0.000	0.033	0.000	0.031	0.002	0.034	0.002
Ile	218	0.038	0.038	0.091	0.091	0.068	0.049	0.203	0.101
Glu	156	0.010	0.001	0.014	0.004	0.020	0.009	0.022	0.007
Glycerate	292	1.676	0.636	1.922	0.653	<b><u>3.521</u></b>	<b><u>0.069</u></b>	3.609	0.746
Lactate	117	0.111	0.075	0.421	0.033	0.344	0.172	0.268	0.163
Glycerol	293	0.072	0.041	0.081	0.043	0.075	0.055	0.114	0.018
Succ	172	0.176	0.080	0.283	0.100	<b><u>0.752</u></b>	<b><u>0.154</u></b>	<b><u>0.506</u></b>	<b><u>0.044</u></b>
Succ	247	0.219	0.071	0.266	0.102	<b><u>0.954</u></b>	<b><u>0.071</u></b>	<b><u>0.607</u></b>	<b><u>0.039</u></b>
Mal	233	0.040	0.001	0.053	0.010	<b><u>0.100</u></b>	<b><u>0.001</u></b>	0.041	0.002
Fum	245	0.098	0.026	0.084	0.014	0.094	0.033	0.128	0.019
GABA	174	0.015	0.003	0.024	0.008	nd	nd	nd	nd
Erythritol	217	0.425	0.130	0.438	0.149	2.212	1.808	1.207	0.871
Sucrose	437	0.000015	0.000007	0.000018	0.000009	0.000104	0.000068	0.000036	0.000010

**Table S10. Total <sup>13</sup>C-enrichment in primary metabolites.** Experimental and statistical analysis as described in the Table S9.

Metabolite	Total <sup>13</sup> C enrichment								
	m/z	M30	SE	M60	SE	GC30	SE	GC60	SE
Gly	102	3257	1665	4837	624	1083	496	4738	997
Ser	306	71.7	22.1	194.9	40.0	135.6	90.9	<u>303.9</u>	<u>23.4</u>
Ser	204	1642	976	1786	579	921	332	836	103
Homoserine	128	1524	976	628	44	1331	526	2202	1073
Glycolate	205	658	658	646	646	1212	609	1370	595
Val	218	30.3	7.2	20.9	13.7	<u>7.3</u>	<u>4.7</u>	13.2	0.9
Ala	188	694	513	715	335	479	228	69	36
Thr	219	276	105	270	75	136	38	128	13
Thr	291	735	253	740	201	400	104	377	49
Pro	142	251	92	186	24	133	50	<u>52</u>	<u>15</u>
Asp	218	12.0	12.0	12.5	12.5	14.8	1.7	8.9	4.7
Asp	232	1533	76	1303	37	<u>2352</u>	<u>133</u>	1154	6
Leu	158	499	23	514	29	<u>386</u>	<u>31</u>	437	33
Ile	218	1.84	1.84	8.88	8.88	2.72	1.36	17.59	7.21
Glu	156	6938	109	6594	2023	<u>2249</u>	<u>566</u>	2423	313
Glycerate	292	92.6	37.0	78.0	15.7	39.9	0.3	47.9	8.9
Lactate	117	356	251	148	13	349	130	500	230
Glycerol	293	3363	1273	2824	992	5972	2954	1522	283
Succ	172	5380	3759	1361	336	779	246	905	165
Succ	247	303	88	226	64	<u>87</u>	<u>12</u>	134	22
Mal	233	1341	31	1790	330	<u>3242</u>	<u>41</u>	1289	53
Fum	245	713	241	651	113	548	179	529	19
GABA	174	14330	2650	9640	3556	nd	nd	nd	nd
Erythritol	217	206	53	186	43	133	64	<u>60</u>	<u>15</u>
Sucrose	437	477177	82661	607521	270298	427991	174100	486175	190880

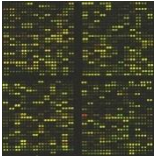
**Table S11. <sup>13</sup>C-enrichment in primary metabolites.** Experimental and statistical analysis as described in Table S9.

Metabolite	13C enrichment								
	<i>m/z</i>	M30	SE	M60	SE	GC30	SE	GC60	SE
Gly 2TMS	102	4.7	0.2	5.1	0.1	3.6	0.7	5.0	0.2
Ser	306	0.8	0.5	1.1	0.2	1.0	0.6	<u>3.3</u>	<u>0.1</u>
Ser	204	8.9	0.6	9.2	0.4	8.9	0.5	8.9	0.2
Homoserine	128	16.1	0.3	15.4	0.1	15.9	0.5	<u>16.5</u>	<u>0.0</u>
Glycolate	205	2.3	2.3	2.1	2.1	4.3	2.1	4.8	2.1
Val	218	2.5	1.3	1.3	1.1	0.6	0.3	1.5	0.2
Ala	188	9.4	1.5	12.1	4.2	12.8	1.4	5.1	2.9
Thr	219	8.9	0.2	8.5	0.1	9.1	0.4	<u>8.9</u>	<u>0.0</u>
Thr	291	21.6	0.5	21.2	0.3	22.5	0.1	22.4	0.5
Pro	142	5.6	0.1	5.4	0.0	<u>5.3</u>	<u>0.0</u>	4.3	0.6
Asp	218	0.5	0.47	0.4	0.39	<u>4.4</u>	<u>1.4</u>	2.3	1.3
Asp	232	8.3	0.6	7.0	0.3	<u>13.5</u>	<u>0.8</u>	6.6	0.1
Leu	158	4.1	0.1	4.1	0.1	<u>3.5</u>	<u>0.3</u>	3.9	0.2
Ile	218	0.3	0.3	0.9	0.9	0.4	0.2	1.9	0.9
Glu	156	6.3	1.6	7.8	0.4	5.1	2.4	<u>5.0</u>	<u>1.0</u>
Glycerate	292	10.5	0.3	11.4	0.6	<u>11.9</u>	<u>0.1</u>	12.6	0.1
Lactate	117	5.3	2.6	7.9	0.6	8.8	0.2	8.1	0.2
Uracil	241	5.2	0.2	5.6	0.5	<u>7.1</u>	<u>0.0</u>	6.4	0.2
Uracil	255	9.1	0.1	9.3	0.1	<u>10.8</u>	<u>0.4</u>	<u>10.8</u>	<u>0.1</u>
Adipic acid	111	1.9	0.1	1.9	0.1	1.8	0.0	2.1	0.1
Adipic acid	141	6.0	0.6	5.9	0.2	6.0	0.3	6.5	0.3
Threonate	292	10.0	0.2	10.1	0.4	6.5	3.7	nd	nd
Salicylic acid	267	8.8	1.2	9.3	1.1	nd	nd	nd	nd
Glycerol	293	12.1	0.6	12.0	0.5	12.4	0.1	12.8	0.2
OXA	175	nd	nd	nd	nd	14.5	0.3	nd	nd
Succ	172	22.6	6.1	17.8	0.5	22.5	1.7	<u>21.0</u>	<u>1.1</u>
Succ	247	7.3	0.5	6.9	0.3	<u>9.0</u>	<u>0.3</u>	<u>9.0</u>	<u>1.0</u>
Mal	233	7.3	0.0	9.7	1.8	<u>18.0</u>	<u>0.1</u>	7.3	0.3
Citramalate	247	0.3	0.28	0.1	0.097	0.8	0.4	<u>1.3</u>	<u>0.8</u>
Fum	245	7.6	0.4	7.2	0.0	6.7	1.6	8.2	0.5
GABA	174	6.6	0.1	6.4	0.1	nd	nd	nd	nd
Erythritol	217	8.6	0.2	8.3	0.2	9.3	1.0	6.6	1.8
myo inositol	191	4.9	4.9	4.8	4.8	7.2	4.1	11.6	2.1
Sucrose	437	2.5	0.8	2.5	0.1	<u>4.7</u>	<u>0.3</u>	<u>3.7</u>	<u>0.4</u>
Trehalose	169	3.9	2.2	5.6	2.8	5.1	2.7	5.0	2.5
Maltose	361	7.6	3.8	8.7	2.2	nd	nd	8.1	0.3
Isomaltose	361	nd	nd	12.6	0.6	nd	nd	nd	nd

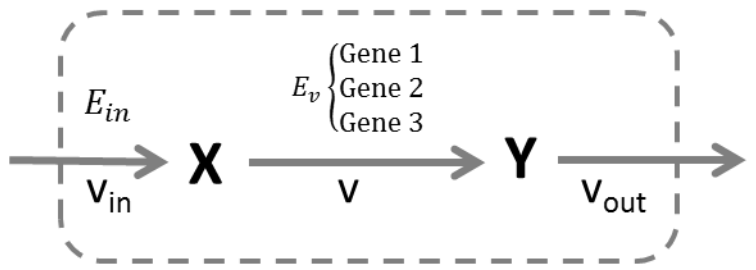
**Table S12. Content of the metabolites analyzed in this study.** The content (ng) of each metabolite was obtained using the equation of a linear regression of the peak area obtained from different concentrations of standard compounds.

Metabolite	Concentration (ng)							
	M30	SE	M60	SE	GC30	SE	GC60	SE
Gly	675.1	319.4	949.3	103.7	266.1	84.7	959.5	238.7
Ser	171.7	94.6	189.2	55.6	100.6	32.8	93.5	9.3
Homoserine	92.3	57.6	40.9	2.8	81.7	30.6	133.6	65.2
Glycolate	291.5	7.3	290.9	6.1	283.0	4.0	284.3	2.8
Val	17.1	4.7	29.4	8.4	9.6	2.1	9.3	0.7
Ala	71.7	54.4	58.7	32.7	42.1	22.1	23.4	8.4
Thr	34.5	12.5	34.8	9.3	17.8	4.7	16.8	1.8
Pro	44.2	15.9	34.3	4.3	24.8	9.4	<b><u>11.7</u></b>	<b><u>2.0</u></b>
Asp	184.4	3.9	187.1	3.9	<b><u>174.1</u></b>	<b><u>0.9</u></b>	<b><u>175.0</u></b>	<b><u>1.5</u></b>
Leu	120.6	2.3	124.9	3.7	111.3	0.8	112.8	1.5
Ile	17.2	6.2	22.5	6.3	9.9	2.8	10.0	0.7
Glu	673.4	207.5	697.1	263.6	224.6	92.0	324.1	146.4
Glycerate	8.9	3.7	7.0	1.7	3.4	0.0	3.8	0.7
Lactate	46.4	29.2	18.7	0.9	40.1	15.5	60.7	27.5
Salicylic acid	10.7	7.6	5.3	2.2	0.5	0.1	0.5	0.1
Glycerol	289.4	118.7	243.6	93.2	482.3	239.2	118.2	20.1
Succ	192.6	93.8	77.4	20.6	33.3	8.4	42.5	5.7
Mal	182.9	4.3	184.3	1.1	179.6	1.9	177.7	0.1
Fum	94.9	33.1	90.4	15.7	81.0	22.4	<b><u>65.8</u></b>	<b><u>7.0</u></b>
GABA	489.1	97.1	343.7	120.0	<b><u>135.4</u></b>	<b><u>78.2</u></b>	<b><u>35.2</u></b>	<b><u>20.3</u></b>
Erythritol	24.1	6.6	22.7	5.5	15.8	8.0	11.5	4.7
Sucrose	246540	86181	239692	101307	97619	43785	124067	39544

# 1) Preprocess data



gene name – RMA value  
 Gene 1– 1.1  
 Gene 2– 1.4  
 Gene 3 – 1.5



RMA (affy R package)

Affymetrix probe names → Arabidopsis gene names



# 2) Map data to reactions

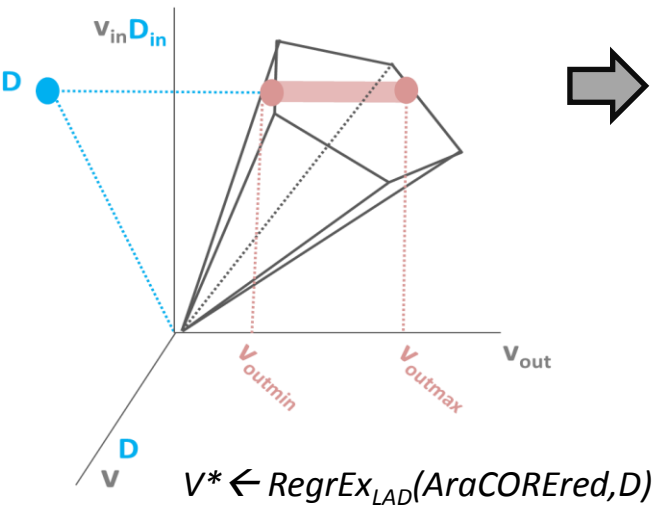
**Ev rule:** Gene 3 OR Gene 1 OR (Gene 3 AND Gene 2) OR (Gene 1 AND Gene 2)

**Dv:** max(Gene 3, Gene 1, min(Gene 3, Gene 2), min(Gene 1, Gene 2)) = 1.5

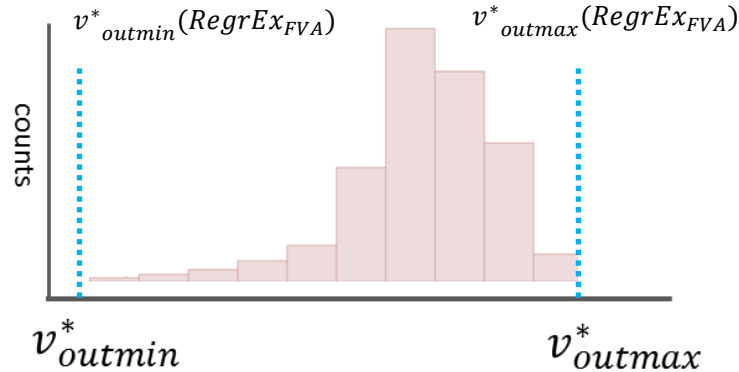
$D \leftarrow \text{mapgene2rxn}(\text{GPR rules, gene names, RMA value})$



# 3) Obtain cell-specific flux distribution



# 4) Obtain AO space sample

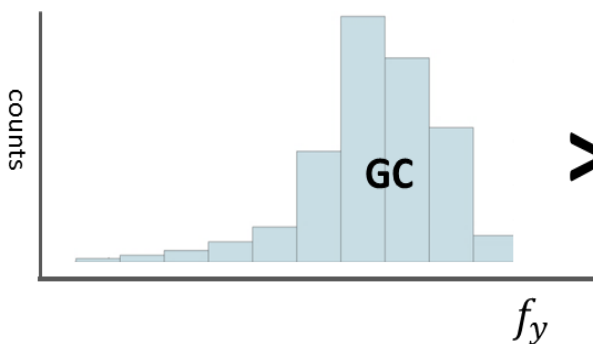


$V_{AO} \leftarrow \text{RegrEx}_{AOS}(\text{AraCOREred}, D, V^*)$



# 5) Obtain flux-sum distributions per metabolite and compare between cell-types

$h_1$  (MWW test,  $\alpha = 0.05$ ):



>

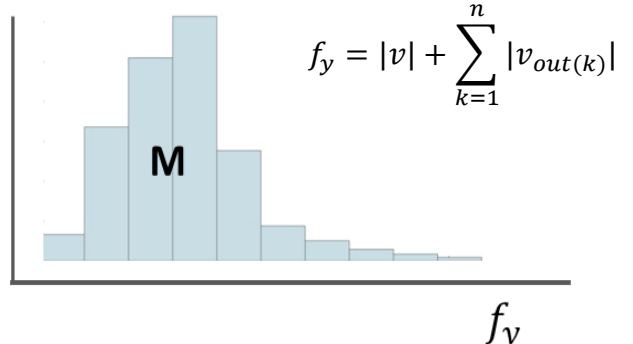


**Figure S1. Schematic depiction of the workflow followed to obtain metabolic predictions specific to G and M cells.** This schematic depiction is based on the toy metabolic model displayed in the top right: X first enters the system through the reaction,  $v_{in}$ , which is dependent on the transporter  $E_{in}$ . X is then transformed to Y through  $v$ , which is dependent on  $E_v$  (coded by gene1-3). Finally Y diffuses spontaneously to the exterior ( $v_{out}$ ), and hence no genes are associated to this reaction. (1) In a first step, expression data is preprocessed, which includes data RMA normalization and mapping of array probe names to (Arabidopsis) gene names. (2) Gene expression values are then mapped to reactions in the metabolic model following the gene-protein-reaction rules contained in the model, which generates the vector D of mapped expression values. (3) In a third step, a cell-specific flux distribution that is closest to the mapped expression data integrated in the metabolic model is obtained through  $RegrEx_{LAD}$ . However, the optimal solution (*i.e.*, flux distribution) is not unique, and an alternative optima space (AO) exists. In this case, this is because D contains data to only two of the three reactions ( $v_{in}$  and  $v$ ) since  $v_{out}$  has not associated gene-protein-reaction rule. Thus,  $v_{out}$  can vary in an orthogonal direction to the plane, where D lies, without affecting the optimal value of the  $RegrEx_{LAD}$  objective function (see Appendix S1). (4) To account for this issue, the AO space is sampled through  $RegrEx_{AOS}$  and a sampled distribution of optimum flux values for  $v_{out}$  is obtained. Additionally, the function  $RegrEx_{FVA}$  calculates the minimum and maximum values in the alternative optima space, as a means to validate the coverage of the random sample. (5) Finally, flux-sums are calculated for each metabolite across the previously obtained AO sample (here only depicted for the case of Y), thus obtaining another distribution of flux-sums. This process is applied to the two cell types, G and M cells, and the resulting AO flux and flux-sum distributions are compared through a Mann-Whitney-Wilcoxon (MWW) test. In this example, the alternative hypothesis (H1) states that the flux-sum distribution corresponding to G cells is greater than that of M cells, while the null hypothesis states that both distributions are indistinguishable. Here, the null hypothesis is rejected at a significant level of  $\alpha = 0.05$ .

## Appendix S1. A brief description of the ReGrEx Alternative Optima Sampling method used in this study

ReGrEx<sup>1</sup> finds the optimal flux distribution within the flux cone,  $v_{opt} \in \mathcal{C} = \{v: Sv = 0, v_{min} \leq v \leq v_{max}\}$ , that minimizes the second norm of the difference vector  $\epsilon = d - |v|$ , where  $d$  represents the data vector used ( $\epsilon$  is defined only over the set of reactions with associated data,  $R_D$  in  $OP_1$ ). This is achieved through the mixed integer quadratic program displayed in  $OP_1$ . The introduction of the vector of binary variables,  $x$ , is required to cope with the absolute values (*i.e.*,  $|v|$ ) in  $\epsilon$  in a manner that guarantees the computational tractability of the optimization problem. To this end, reversible reactions in  $v$  are split into the forward and backward direction ( $v_{for}$  and  $v_{back}$ , respectively) and forced to take non-negative values and be mutually exclusive (*i.e.* for each reversible reaction  $i$ ,  $v_{for(i)} \geq 0 \text{ XOR } v_{back(i)} \geq 0$ ), as ensured by constraints 6-9 in  $OP_1$ .

$$\begin{aligned}
 v_{opt} &= \arg \min_{\substack{\epsilon = [\epsilon_{irr}; \epsilon_{for}; \epsilon_{back}] \in \mathbb{R} \\ v = [v_{irr}; v_{for}; v_{back}] \in \mathbb{R}_0^+ \\ x \in \{0,1\}^n}} \frac{1}{2} \|\epsilon\|_2^2 + \lambda \|v\|_1 \\
 \text{s.t.} \\
 1. & Sv = 0 \\
 2. & v_{irr_i} + \epsilon_{irr} = d_{irr} \\
 3. & v_{for_i} + \epsilon_{for} - x_i d_{rev} = d_{rev} \\
 4. & v_{back_i} + \epsilon_{back} - x_i d_{rev} = 0 \\
 5. & v_{irr \min} \leq v_{irr} \leq v_{irr \max} \\
 6. & v_{for} + xv_{for \min} \geq v_{for \min} \\
 7. & v_{back} - xv_{back \min} \geq 0 \\
 8. & v_{for} + xv_{for \max} \leq v_{for \max} \\
 9. & v_{back} - xv_{back \max} \leq 0
 \end{aligned} \quad \left. \vphantom{\begin{aligned} 2. \\ 3. \\ 4. \end{aligned}} \right\} \quad i \in R_D \quad (OP_1).$$

In addition to the second norm of  $\epsilon$ , a penalty term weighted by parameter  $\lambda$  is added to the objective function. This penalty term corresponds to the first norm of the flux vector,  $v$ , which controls the sparsity in  $v_{opt}$  as a means to eliminate reactions that are not important (as determined by the used expression data) to a given context.

In this study, we have slightly modified the objective function in  $OP_1$ . Concretely, we minimized the first norm of  $\epsilon$  instead of its second norm. This change converts the previous mixed integer quadratic program to the mixed integer linear program displayed in  $OP_2$ .

$$\begin{aligned}
v_{opt} &= \arg \min w^T (\epsilon^+ + \epsilon^-) + \lambda \|v\|_1 \\
\epsilon^+ &= [\epsilon_{irr}^+, \epsilon_{for}^+, \epsilon_{back}^+], \\
\epsilon^- &= [\epsilon_{irr}^-, \epsilon_{for}^-, \epsilon_{back}^-], \\
v &= [v_{irr}, v_{for}, v_{back}] \in \mathbb{R}_0^+, \\
x &\in \{0,1\}^n \\
s.t. \\
1. & S_{ext} v = 0 \\
2. & v_{irr_i} + (\epsilon_{irr}^+ - \epsilon_{irr}^-) = d_{irr} \\
3. & v_{for_i} + (\epsilon_{for}^+ - \epsilon_{for}^-) + x d_{rev} = d_{rev} \\
4. & v_{back_i} + (\epsilon_{back}^+ - \epsilon_{back}^-) - x d_{rev} = 0 \\
5. & v_{irr_{min}} \leq v_{irr} \leq v_{irr_{max}} \\
6. & v_{for} + x v_{for_{min}} \geq v_{for_{min}} \\
7. & v_{back} - x v_{back_{min}} \geq 0 \\
8. & v_{for} + x v_{for_{max}} \leq v_{for_{max}} \\
9. & v_{back} - x v_{back_{max}} \leq 0 \\
10. & r_{lb} v_O - v_C \leq 0 \\
11. & r_{ub} v_O - v_C \geq 0
\end{aligned} \quad \left. \vphantom{\begin{aligned} 2. \\ 3. \\ 4. \end{aligned}} \right\} \quad i \in R_D \quad (OP_2).$$

The first norm of  $\epsilon$  involves absolute values (*i.e.*,  $\|\epsilon\|_1 = \sum_i |\epsilon_i|$ ), which cannot be directly treated in conventional numerical solvers. A way to computationally deal with this consist of splitting  $\epsilon$  into two non-negative terms (*i.e.*  $\epsilon = \epsilon^+ - \epsilon^-$ ). Hence,  $\|\epsilon\|_2^2$  is replaced by  $\epsilon^+ + \epsilon^-$  in the objective function of  $OP_2$ . In addition, a vector  $w$ , weighting the contribution of each element in  $\epsilon$ , was introduced in the objective function. Concretely, each element  $w_i = \sigma_i^{-1}$  was defined as the inverse value of the standard deviation  $\sigma_i$  of the gene expression among the three replicates available for each cell type that was associated to reaction  $i$ . The last two constraints (10 and 11) impose the constraint on the carboxylation to oxygenation ratio discussed in the main text, *i.e.*  $r_{lb} \leq \frac{v_C}{v_O} \leq r_{ub}$ .

Finally, the development of the modified RegrEx version (called RegrEX<sub>LAD</sub>, for least absolute deviations) presented in  $OP_2$  was motivated to facilitate the computational tractability of the alternative optima space associated to the data integration problem (next section).

## Evaluation of the alternative optima space

When integrating expression data into a genome-scale model, an alternative optima space,  $V_{AO}$ , of optimal flux distributions,  $v_{opt}$ , may exist. Concretely, when using  $OP_2$  for the data integration, the elements of  $V_{AO}$  share the same objective function value and satisfy all imposed constraints, that is,  $V_{AO} = \{v_{opt} : \|\epsilon\|_1 + \lambda \|v_{opt}\|_1 = Z_{opt}, S v_{opt} = 0, v_{min} \leq v_{opt} \leq v_{max}\}$ . The main cause of this alternative optimal space of solutions can be attributed to the existence of reactions in a genome-scale model that do not contain associated gene expression data. This subsequently implies that there are reactions whose flux can vary without affecting the value of  $Z_{opt}$ .

We used a recently developed method<sup>2</sup>, to analyze the alternative optima space associated to the data integration in AraCOREd. RegrEX<sub>AOS</sub> (RegrEx Alternative Optima Sampling) was

designed to generate a uniform sample of the alternative optima space associated to  $\text{RegrEx}_{\text{LAD}}$ . To this end, it first generates a random flux vector,  $v_{\text{rand}}$ , and then searches for the closest flux distribution,  $v \in V_{\text{AO}}$ , to  $v_{\text{rand}}$  that belongs to the alternative optima space of the previous  $\text{RegrEx}_{\text{LAD}}$  optimization. This is accomplished through the mixed integer linear program depicted in  $\text{OP}_3$  (this process is repeated  $n$  times to obtain the uniform sample).

$$\begin{aligned}
& \min && \| \delta^+ + \delta^- \|_1 \\
& \epsilon^+ = [\epsilon_{\text{irr}}^+, \epsilon_{\text{for}}^+, \epsilon_{\text{back}}^+ ], \\
& \epsilon^- = [\epsilon_{\text{irr}}^-, \epsilon_{\text{for}}^-, \epsilon_{\text{back}}^- ], \\
& \delta^+ = [\delta_{\text{irr}}^+, \delta_{\text{for}}^+, \delta_{\text{back}}^+ ], \\
& \delta^- = [\delta_{\text{irr}}^-, \delta_{\text{for}}^-, \delta_{\text{back}}^- ], \\
& v = [v_{\text{irr}}, v_{\text{for}}, v_{\text{back}} ] \in \mathbb{R}_0^+, \\
& x \in \{0,1\}^n \\
& \text{s.t.} \\
& 1-11 \quad (\text{OP}_2) \\
& 12. w^T (\epsilon^+ + \epsilon^-) = w^T (\epsilon_{\text{opt}}^+ + \epsilon_{\text{opt}}^-) \\
& 13. \| v \|_1 = \| v_{\text{opt}} \|_1 \\
& 14. v_{\text{irr}} - (\delta_{\text{irr}}^+ - \delta_{\text{irr}}^-) = v_{\text{rand}(\text{irr})} \\
& 15. v_{\text{for}} - (\delta_{\text{for}}^+ - \delta_{\text{for}}^-) - xv_{\text{rand}(\text{rev})} = 0 \\
& 16. -v_{\text{back}} + \delta_{\text{back}} + xv_{\text{rand}(\text{rev})} = v_{\text{rand}(\text{rev})}
\end{aligned} \tag{OP}_3.$$

$\text{OP}_3$  inherits constraints 1-11 from  $\text{OP}_2$  and introduces two sets of new constraints. One set is formed by constraints 12 and 13, and guarantees that the sampled flux distribution shares the same objective value than the previously found  $v_{\text{opt}}$  in  $\text{OP}_2$ . The other set consists of constraints 14-16 introducing the auxiliary variables  $\delta = \delta^+ - \delta^- = v_{\text{rand}} - v_{\text{opt}}^*$ , which measure the distance of an alternative optimum flux distribution to the randomly generated  $v_{\text{rand}}$ . In addition,  $\delta$  is partitioned into the set of irreversible and the forward and reverse directions of reversible reactions, which simplifies the computation of the first norm of  $\delta$  in the objective function.

In addition to generating a sample of alternative optima flux distributions with  $\text{RegrEx}_{\text{AOS}}$ , we also developed a complementary approach to evaluate the extreme flux values within the alternative optima space. This approach, akin to the Flux Variability Analysis<sup>3</sup> procedure, minimizes and maximizes the flux  $v_j$  through each reaction  $j$  in the genome-scale metabolic model such that the flux distribution remains in the alternative optima space, that is,  $v \in V_{\text{AO}}$ . Computing the extreme flux values within the alternative optima space serves to assess the quality of the sampling performed by  $\text{RegrEx}_{\text{AOS}}$ . Concretely, it allows evaluating whether the sample covers the whole range of flux values within the alternative optima space—*i.e.*, it is uniform. This evaluation is importance, since a sample covering the whole allowable range renders not only statistically significant, but also quantitatively accurate results. This is fundamental when comparing alternative optimal distributions of flux values between different metabolic contexts. Our complementary approach, which we term  $\text{RegrEx}_{\text{FVA}}$  ( $\text{RegrEx}$  Flux Variability Analysis), iterates the mixed integer linear program in  $\text{OP}_4$  through each reaction  $j$  in the metabolic model (one time minimizing  $v_j$ , the other maximizing it).

Constraints 1-11 are again inherited from  $OP_1$ , and constraints 12 and 13, which ensure  $v \in V_{AO}$ , are identical to the corresponding ones in  $OP_3$ .

$$\begin{aligned}
 & \min / \max \quad v_j \\
 & \epsilon^+ = [\epsilon_{irr}^+, \epsilon_{for}^+, \epsilon_{back}^+], \\
 & \epsilon^- = [\epsilon_{irr}^-, \epsilon_{for}^-, \epsilon_{back}^-], \\
 & v = [v_{irr}, v_{for}, v_{back}] \in \mathbb{R}_0^+, \\
 & x \in \{0,1\}^n \\
 & \text{s.t.} \\
 & 1-11 \quad (OP_2) \qquad \qquad \qquad (OP_4). \\
 & 12. \quad w^T (\epsilon^+ + \epsilon^-) = w^T (\epsilon_{opt}^+ + \epsilon_{opt}^-) \\
 & 13. \quad \|v\|_1 = \|v_{opt}\|_1
 \end{aligned}$$

### References:

1. Robaina Estévez, S. & Nikoloski, Z. Context-Specific Metabolic Model Extraction Based on Regularized Least Squares Optimization. *PLoS One* **10**, e0131875 (2015).
2. Robaina Estévez, S. & Nikoloski, Z. On the effects of alternative optima in context-specific metabolic model predictions. *Plos Comp.Biol. In Press.* (2017).
3. Mahadevan, R. & Schilling, C. H. The effects of alternate optimal solutions in constraint-based genome-scale metabolic models. *Metab. Eng.* **5**, 264–276 (2003).